Supplementary Information (SI) for Journal of Materials Chemistry A.

Supplementary Information

Photosensitization by $[Mo_3S_{13}]^{2-}$ nanocluster cocatalysts enabling visible-light photocatalytic H_2 evolution

Chao Yang,[abc] Xiao-Li Pu,[abc] Qi Yin,[bc] Qing-Ping Huang,[bc] Lei Cai,*[d] Ping Liu[a] and Zhi-Bin Fang*[abc]

[a] *College of Chemistry, Fuzhou University, Fuzhou 350108, P. R. China*

[b] *State Key Laboratory of Structural Chemistry, Fujian Institute of Research on the Structure of Matter, Chinese Academy of Sciences, Fuzhou, 350108, P. R. China*

[c] *Fujian College, University of Chinese Academy of Sciences, Fuzhou 350002, P. R. China.*

[d] *College of Chemistry and Chemical Engineering, Xinjiang Agricultural University, Urumqi 830052, P. R. China.*

*Corresponding authors: fangzhibin@fjirsm.ac.cn; lcai@xjau.edu.cn

Characterizations

Crystal structure identification was performed using Bruker D8 Advance X-ray diffractometer (XRD) with Cu Kα radiation ($\lambda = 0.15418$ nm) operating at 40 kV and 40 mA. Scanning electron microscopy (SEM) images were obtained using a HITACHI SU8000 field-emission scanning electron microscope. Transmission electron microscopy (TEM) images were taken on a Tecnai G2 F20 S-TWIN (FEI company). UV-Vis diffuse reflectance spectroscopy (DRS) was measured by a Carry 500 UV-Vis spectrophotometer using $BaSO_4$ as the background. Zeta potential was measured by a Zetasizer Nano ZEN3690 (Malvern Instruments. Ltd) using a DTS1070 cuvette dispersed in solvents at 25℃. Raman spectroscopy was performed on a microscopic confocal laser Raman spectrometer (inVia Reflex, Renishaw Co.) using a $\lambda = 532$ nm laser at room temperature. Bruker model A300 spectrometer (frequency: 9.86 GHz; central field: 3512.48 G) was used to detect the electron paramagnetic resonance (EPR) signals of samples. X-ray photoelectron spectroscopy (XPS) was conducted on ESCALAB 250Xi spectrometer (ThermoFisher Scientific Inc). XPS spectra were charge-corrected to the adventitious C 1s peak at 284.8 eV. In-situ XPS was conducted on Proven-X NAP spectrometer (SPECS Surface Nano Analysis GmbH) with additional light irradiation via Xe lamp. The vacuum heating treatments were conducted on ASAP-2020 gas sorption station (Micromeritics Co. Ltd). Ultrafast transient absorption (TA) spectroscopy was tested on samples dispersed in methanol by Helios spectrometer (Ultrafast Systems. Ltd) at a pumping wavelength of 400 nm.

Electrochemical performance tests

The linear sweep voltammetry (LSV), electrochemical impedance spectroscopy (EIS) and photocurrent response were performed on an electrochemical workstation (CHI660E) with a three-electrode system. Ag/AgCl electrode and Pt electrode served as the reference electrode and counter electrode, respectively. Samples deposited in a 0.5×0.5 cm^2 window on ITO glasses served as working electrodes (loading 0.308 $mg\cdot cm^{-2}$) for EIS and photocurrent tests with 0.2 M Na_2SO_4 aqueous solution as the electrolyte. LSV test was carried out in 0.5 M H_2SO_4 electrolyte with scan rate of 10 $mV\cdot s^{-1}$, and samples were loaded on glassy carbon electrodes with 3 mm diameter as working electrodes (loading 0.424 $mg\cdot cm^{-2}$).

Computational method

Two different models were constructed based on a 4×4×1 ZnS supercell. In the model of Figure

5a, a 2×2×1 $(NH_4)_2Mo_3S_{13}$ supercell was placed on the surface. In the model of Figure S14, a single Mo_3S_{13} cluster was placed on the ZnS surface. For both models, the initial adsorption site was chosen as the S-top site of Mo_3S_{13}. The Density Functional Theory (DFT) calculations were performed with Gaussian 16 program[1] and the input files were created by Multiwfn package[2]. The B3LYP hybrid functional[3] and def2-SVP basis set were adopted and the dispersion correction has been considered by using DFT-D3BJ method of Grimme[4] in optimization and single point energy calculations. The difference map for electron density is plotted by the Multiwfn package[2]. and visualized by VESTA software.

Reference

1. M. J. Frisch, G. W. T., H. B. Schlegel, G. E. Scuseria, *et al.*, a. D. J. F., Gaussian, Inc., Wallingford CT, Gaussian 16. **2019**.
2. Lu, T.; Chen, F., Multiwfn: a multifunctional wavefunction analyzer. *J. Comput. Chem.* **2012,** *33*(5), 580-92.
3. Becke, A. D., Density-functional thermochemistry. III. The role of exact exchange. *J. Chem. Phys.* **1993,** *98* (7), 5648-5652.
4. S. Grimme, S. Ehrlich, L. Goerigk, Effect of the damping function in dispersion corrected density functional theory. *J. Comput. Chem.* **2011,** *32* (7), 1456-65.

Results

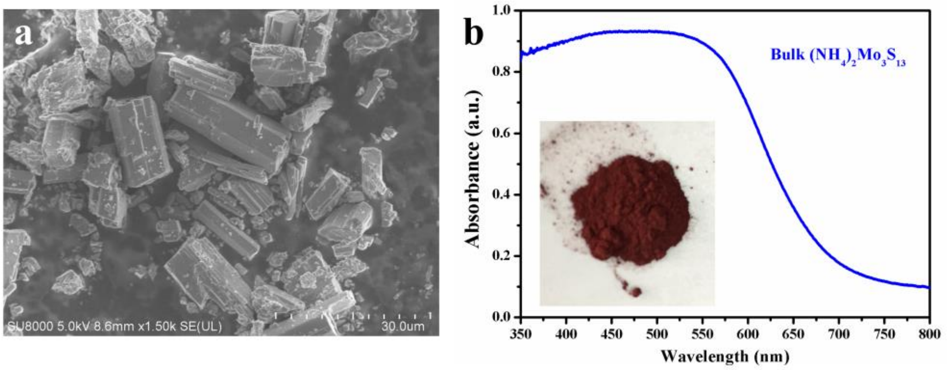

Figure S1 (a) SEM images of as-prepared bulk $(NH_4)_2Mo_3S_{13}$, (b) DRS spectra.

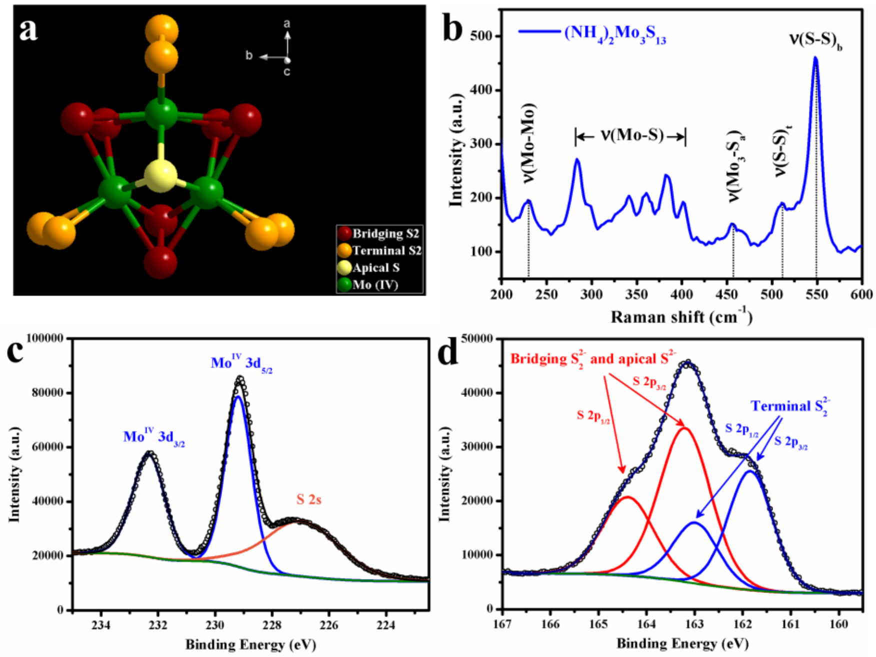

Figure S2 (a) Model of a single $[Mo_3S_{13}]^{2-}$ cluster; (b) Raman spectrum and (c)(d) XPS spectra of as-prepared $(NH_4)_2Mo_3S_{13}\cdot nH_2O$: (c) Mo 3d region; (d) S 2p region.

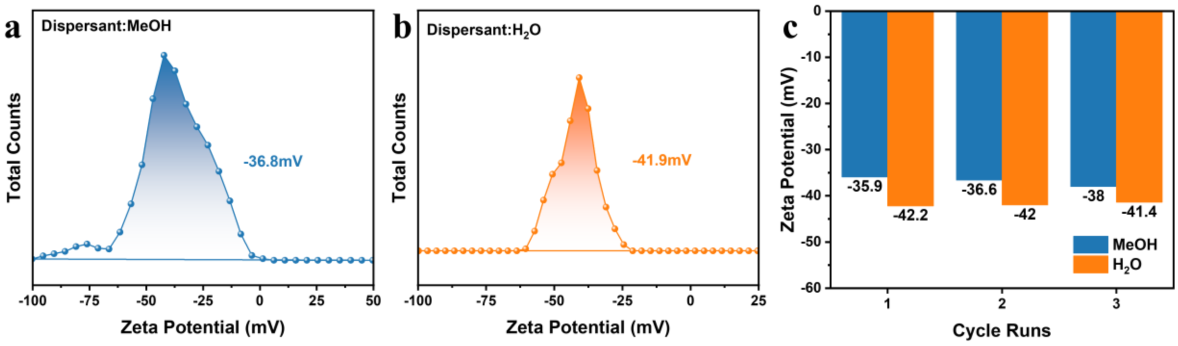

Figure S3 Zeta potentials of $[Mo_3S_{13}]^{2-}$ nanoclusters dispersed in (a) methanol, (b) water, and (c) the values in respective test cycles.

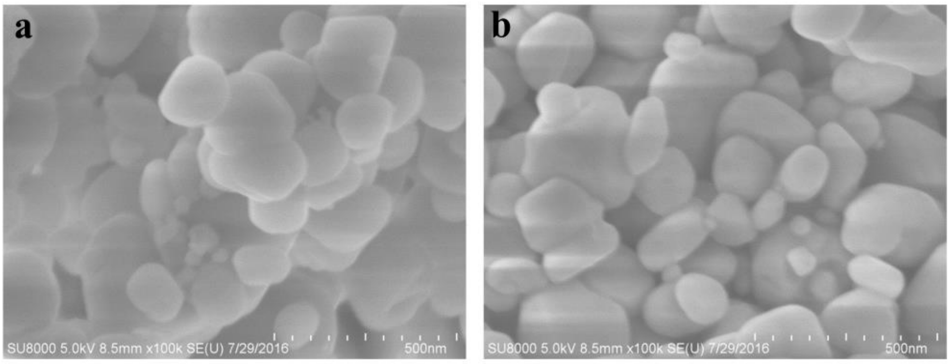

Figure S4 SEM images of (a) C-ZS and (b) 1%M3-C-ZS.

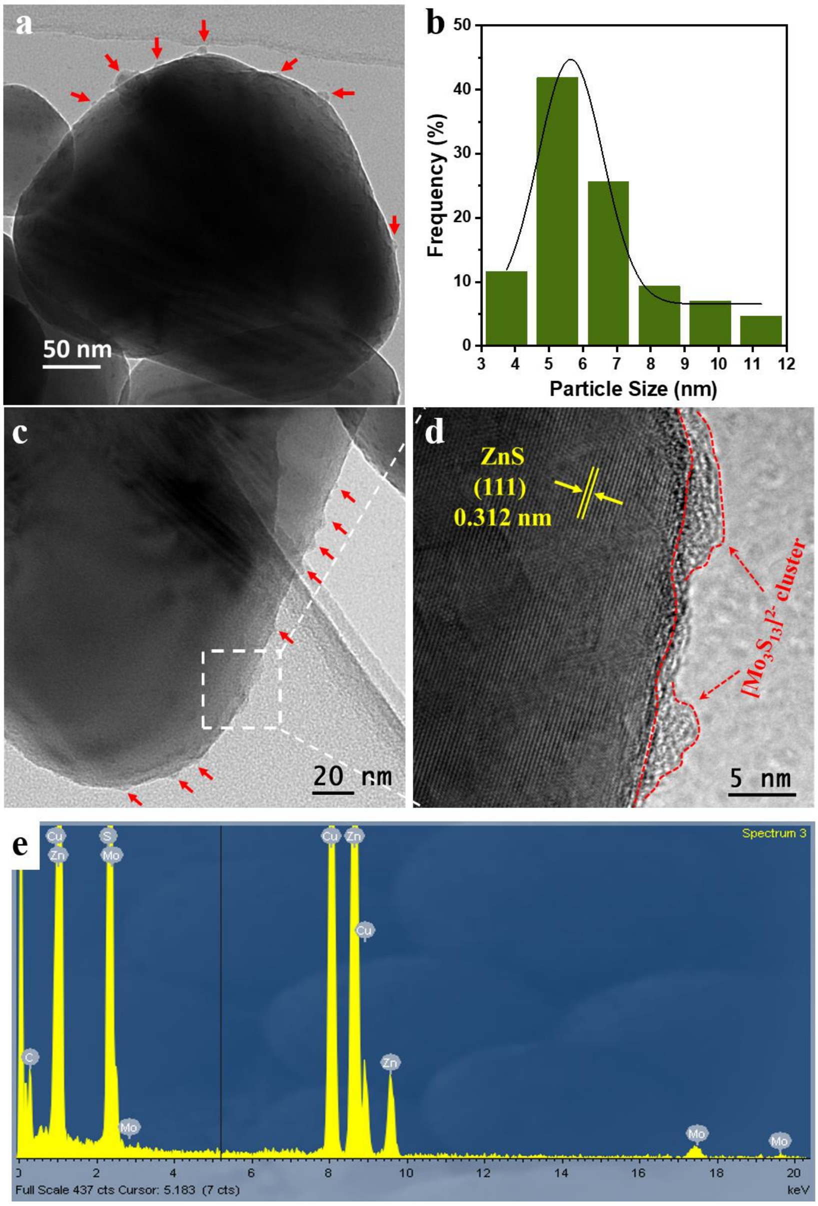

Figure S5 (a)(c) TEM and (d) HRTEM images of 2%M3-C-ZS sample; (b) Size Distribution of supported $[Mo_3S_{13}]^{2-}$ nanoclusters counted from Figures 2d, S5a and S5c; (e) Corresponding EDX spectrum of (a).

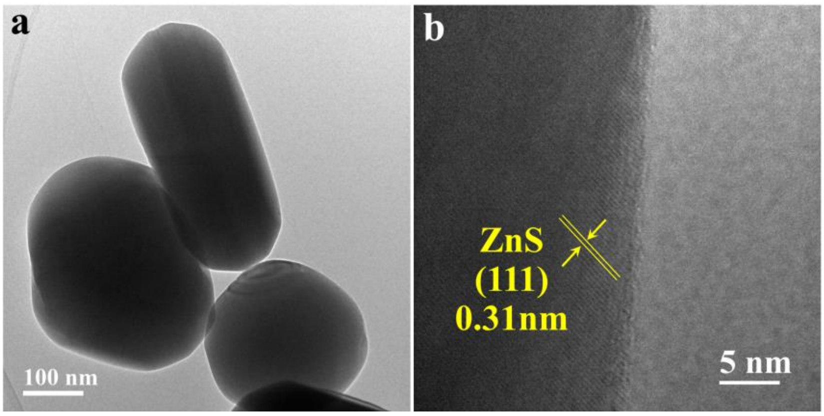

Figure S6 (a) TEM image of C-ZS sample and (b) HRTEM image of the edge of C-ZS nanoparticle.

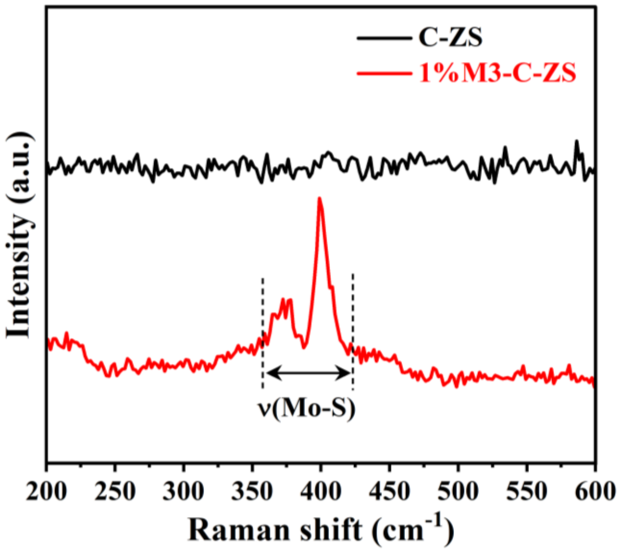

Figure S7 Raman spectra of 1%M3-C-ZS and C-ZS.

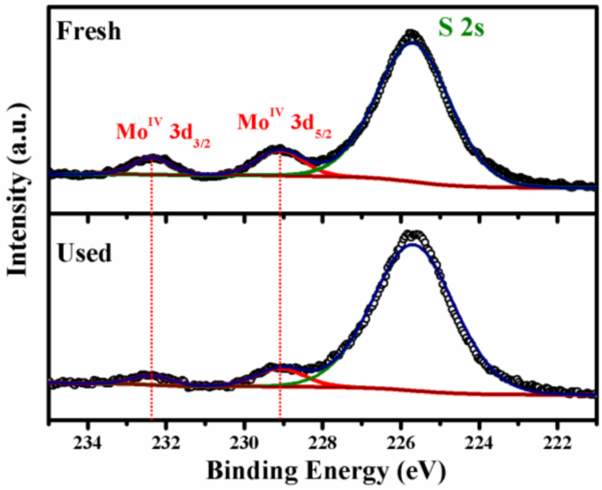

Figure S8 XPS Mo 3d spectra for 1%M3-C-ZS before and after 6 cycle runs of visible-light photocatalysis.

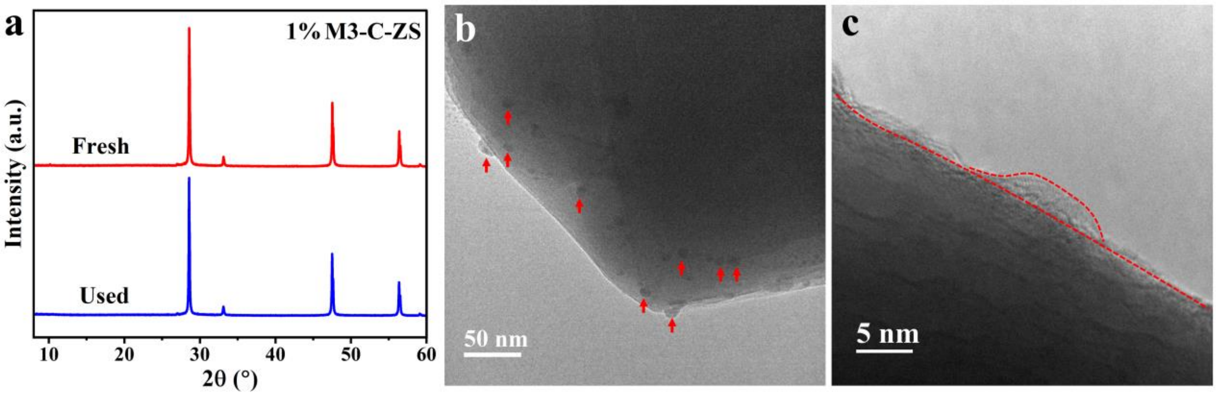

Figure S9 Characterizations of 1%M3-C-ZS after 6 cycle runs of photocatalysis: (a) XRD comparison with fresh sample; (b)(c) TEM images of the used 1%M3-C-ZS.

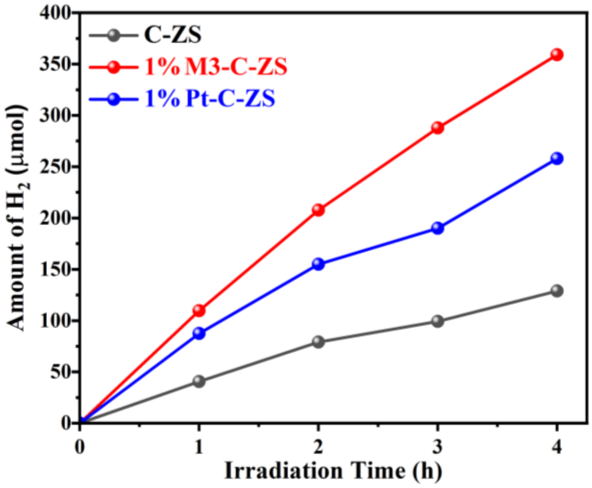

Figure S10 UV-light (300 nm < λ < 400 nm) photocatalytic HER activities of 1%M3-C-ZS (30 mg) compared with C-ZS, and 1%Pt-C-ZS (prepared via in-situ photodeposition of 1%wt Pt on ZnS)

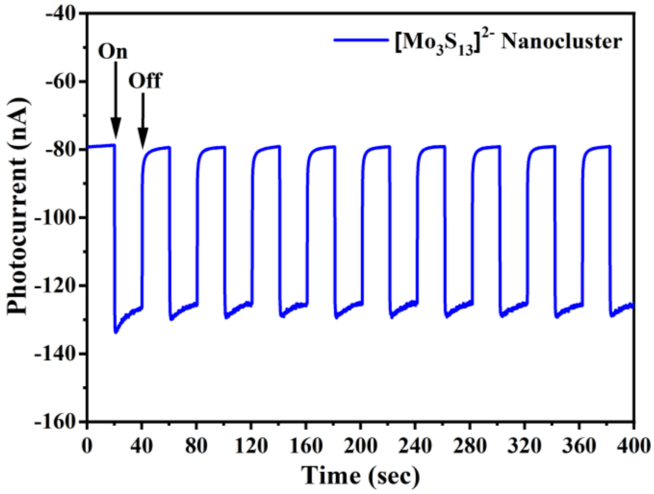

Figure S11 Photocurrent response of sole $[Mo_3S_{13}]^{2-}$ nanoclusters under visible light irradiation (λ ≥ 410 nm, 0 V bias).

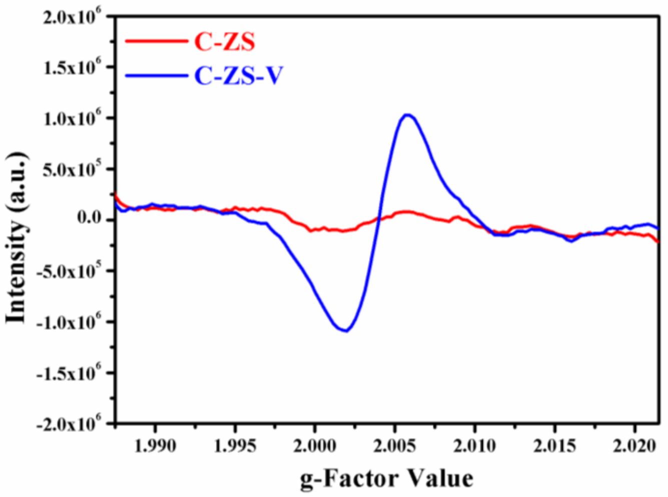

Figure S12 Evidence of defects in ZnS: EPR spectra of C-ZS and C-ZS-V.

Table S1 Data for the calculation of HER AQYs by 30 mg 1%M3-C-ZS photocatalyst.

Wavelength (nm)	**Irradiance[a] ($\mu W \cdot cm^{-2}$)**	**H_2 yield ($\mu mol/h/g_{cat}$)**	**Number of incident photons**	**Number of reacted electrons**	**AQY (‰)**
400	18747.8	19.8	4.9×10^{22}	2.4×10^{19}	0.49
420	19674.9	17.7	5.1×10^{22}	2.1×10^{19}	0.41
450	24129.5	17.4	6.3×10^{22}	2.1×10^{19}	0.33
475	26401.4	12.6	6.9×10^{22}	1.5×10^{19}	0.22
500	27598.1	10.4	7.2×10^{22}	1.2×10^{19}	0.17

[a] The geometric irradiation area of incident lights was 18.08 cm^2.

AQY is defined as the ratio of the number of reacted electrons (2 times of the produced H_2 molecules) to the number of incident photons. The general equation is given below:

$$\text{AQY }(\%) = \frac{Number\ of\ reacted\ electrons}{Number\ of\ incident\ photons} \times 100$$

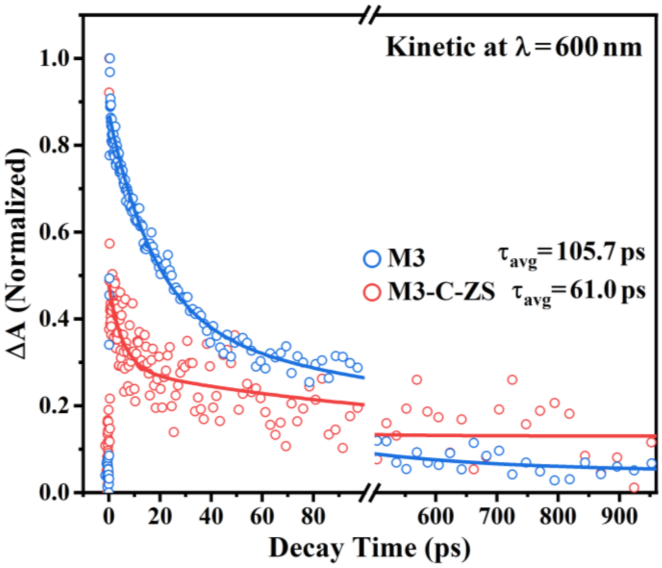

Figure S13 TA kinetics of ESA signal probed at λ = 600 nm.

Table S2 Fitting parameters for the kinetic curves of TA spectra

Sample	**Recovery Time (ps)**		**Amplitude**		**Average τ (ps)**
M3 (at 490 nm)	τ_1	20.76	A_1	0.4155	91.9
	τ_2	162.81	A_2	0.4169	
M3-C-ZS (at 490 nm)	τ_1	4.44	A_1	0.1609	45.2
	τ_2	159.46	A_2	0.0575	
M3 (at 600 nm)	τ_1	18.51	A_1	0.5025	105.7
	τ_2	241.47	A_2	0.3229	
M3-C-ZS (at 600 nm)	τ_1	5.41	A_1	0.1922	61.0
	τ_2	129.56	A_2	0.1558	

$$\tau_{avg} = \frac{\sum_{i=1}^{n} A_i \tau_i}{\sum_{i=1}^{n} A_i}$$

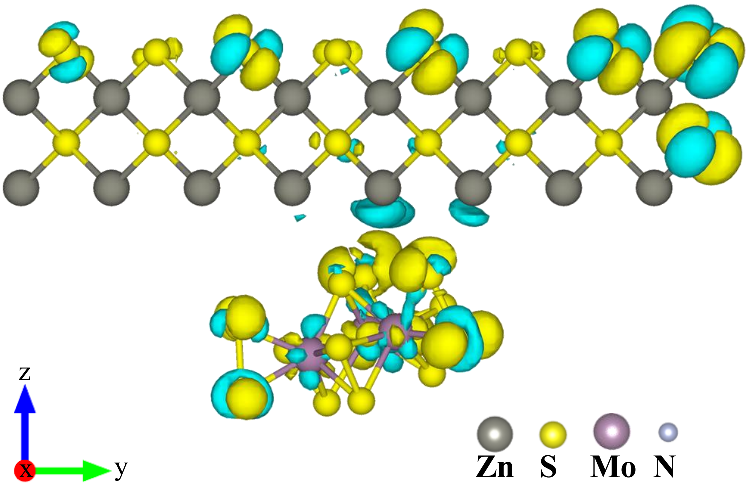

Figure S14 Charge density difference at the interface between single $[Mo_3S_{13}]^{2-}$ cluster and ZnS (cyan: electron gain; yellow: electron loss).